

The synthesis of ferromagnetic $\text{La}_{0.75}\text{Ca}_{0.25}\text{MnO}_3$ nanowires by a sol-gel method

F. E. ATALAY*, V. YAGMUR, S. ATALAY, H. KAYA, S TARI^a, D. AVSAR
Inonu University, Science and Art Faculty, Department of Physics, Malatya 44280, Turkey
^a*IYTE, Science Faculty, Department of Physics, Izmir, Turkey*

In this study, densely packed $\text{La}_{0.75}\text{Ca}_{0.25}\text{MnO}_3$ (LCMO) nanowires were synthesized within a porous anodic aluminum oxide (AAO) template by means of a sol-gel method using nitrate as raw material and ethylene glycol as the chelating agent. It was observed from measurements of hysteresis curves that the magnetic behavior of the LCMO nanowire arrays was strongly dependent on the pH of the solution. As it has been reported that bulk polycrystalline $\text{La}_{0.75}\text{Ca}_{0.25}\text{MnO}_3$ samples have a Curie temperature of 224 K [1], it is interesting to find that nanowires produced at pH 3 show ferromagnetic properties at room temperature

(Received September 14; 2009; accepted February 18, 2010)

Keywords: Manganites, Nanowires, Sol-gel, Ferromagnetism

1. Introduction

The perovskite manganites are well-known compounds because of their colossal magnetoresistive (CMR) and magnetocaloric properties [2-4]. So far, perovskite manganites have been fabricated as a bulk material or as thin or thick films by employing several different techniques such as conventional solid state reaction [4], electroless plating [5], chemical vapor deposition [6] and sol-gel techniques [7]. Nanoparticles and nanowires of perovskite manganites [8,9] have been recently shown to exhibit properties clearly different to those of their bulk form. These materials have attracted much attention due to their significant technological applications in optical [10], electrical [11] and magnetic [12] devices. Recently, much effort has been expended on methods for the synthesis of nanoscale materials of various elements and compounds. Up to now, the synthesis of oxide nanowires has remained challenging [13-15].

Template synthesis based on ordered anodic aluminum oxide (AAO) has attracted much interest because of its wide application in the fabrication of nanodot, nanowire and nanotube arrays [16-24]. So far, $\text{La}_{0.67}\text{Ca}_{0.33}\text{MnO}_3$ [2,9], $\text{La}_{0.8}\text{Ca}_{0.2}\text{MnO}_3$ [13], $\text{La}_{0.5}\text{Ca}_{0.5}\text{MnO}_3$ [14], $\text{La}_{0.825}\text{Sr}_{0.175}\text{MnO}_3$ [15] and $\text{La}_{0.6}\text{Sr}_{0.4}\text{CoO}_3$ [24] nanowires have been produced in ordered Al_2O_3 substrates using template synthesis methods, and their electrical and magnetic properties have been studied. In this paper, we report fabrication of room-temperature ferromagnetic $\text{La}_{0.75}\text{Ca}_{0.25}\text{MnO}_3$ nanowires by a sol-gel template method.

2. Experimental details

The following procedure was used to synthesize the AAO templates with magnetic nanowires inside them.

Firstly, the AAO templates were prepared by the conventional two-step anodic oxidation procedure [25] as reported in our previous work [22]. Aluminum foil (99.99% purity) was used as the anode, with an exposed area of 1 cm^2 . The Al foil was cleaned with HCl, rinsed with distilled water and acetone, then annealed at $500\text{ }^\circ\text{C}$ for 2 hours. The first anodization was performed in 0.3 M oxalic acid at a constant 200 V anodizing voltage at room temperature for 3 hours. The template was immersed in a mixture of 6.0 wt% H_3PO_4 and 1.8 wt% H_2CrO_4 at room temperature for 30 minutes to remove alumina. A second anodic oxidation for 1 hour and wet etching for 30 minutes was carried out using the first-step conditions. Any remaining Al was removed with saturated HgCl_2 .

Secondly, a system was designed for nanowire production. This combined sol-gel synthesis and template preparation of nanomaterials to produce densely packed $\text{La}_{0.75}\text{Ca}_{0.25}\text{MnO}_3$ nanowires. Stoichiometric amounts of $\text{Ca}(\text{NO}_3)_2 \cdot \text{XH}_2\text{O}$, $\text{La}(\text{NO}_3)_3 \cdot 6\text{H}_2\text{O}$ (99.9%) and $\text{Mn}(\text{NO}_3)_2 \cdot \text{XH}_2\text{O}$ (99.9%) were dissolved in 50 ml ethylene glycol. The pH of the solution was adjusted to a value between 2 and 6 by adding 0.1 mM HCl or 0.1 M NaOH by monitoring with a Jenway 3520 pH meter. The solution was stirred at $192\text{ }^\circ\text{C}$ until a gel was formed. Then the gel was poured into a nanoporous AAO template, which was located on a borosilicate filter funnel connected to a vacuum pump via a pipe, as shown Fig. 1. The outside of the borosilicate filter funnel was surrounded by a $50\text{ }^\circ\text{C}$ water bath. The gel was slowly filled through nanoporous AAO template for 30 minutes using the vacuum pump. Finally, the surface of filled nanoporous AAO template was wiped. It was then annealed in air at $400\text{ }^\circ\text{C}$ for 2 hours and then at $700\text{ }^\circ\text{C}$ for 2 hours, with the temperature ramped from room temperature to $400\text{ }^\circ\text{C}$ and then $700\text{ }^\circ\text{C}$ at a rate $2\text{ }^\circ\text{C}/\text{min}$.

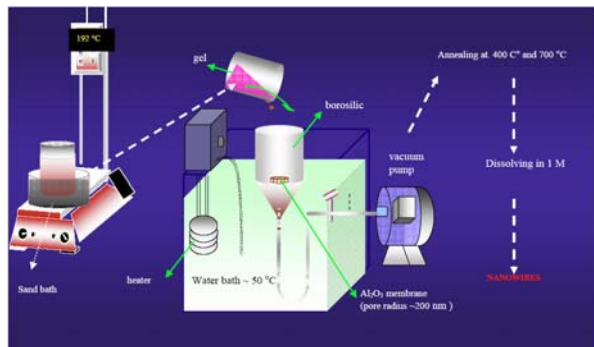


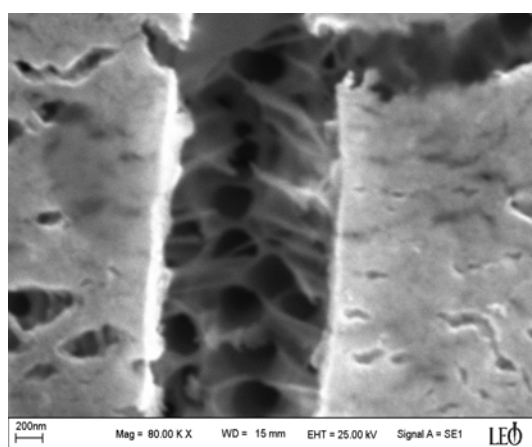
Fig. 1. A representation of the nanowire fabrication process.

The morphology of the nanowire arrays was investigated by scanning electron microscopy (SEM; LEO-EVO-40). The quantitative chemical analyses of the alloys was performed by energy dispersive X-ray (EDX) spectroscopy. X-ray diffraction studies were carried out by

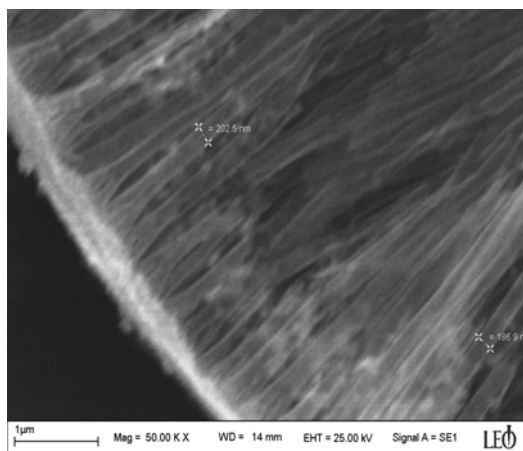
using a Rigaku-Radb diffractometer equipped with $\text{Cu K}\alpha$ radiation. Magnetic measurements were performed with a vibrating sample magnetometer (VSM; Lake Shore 7407) and a Q-3398 (Cryogenic) magnetometer.

3. Results and discussion

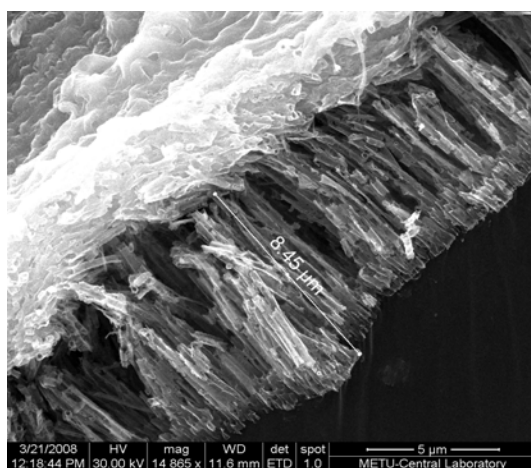
The morphology of the LCMO nanowires obtained in the pores of the Al_2O_3 template is shown in Fig. 2, after different partial dissolution times of the membrane in 1 M NaOH. When the dissolution time was 90 minutes, the nanowires inside the nanopores of the AAO template are parallel, aligned regularly and densely distributed. The average diameter of the nanowires corresponded closely to a pore diameter of 185–195 nm. After a dissolution time of 120 minutes, it was observed that the nanowires were destroyed, as shown in Fig. 2c,d. It is supposed that the nanowires suffer damage by heat treatment of the sol-filled membranes and also the dissolution process itself.



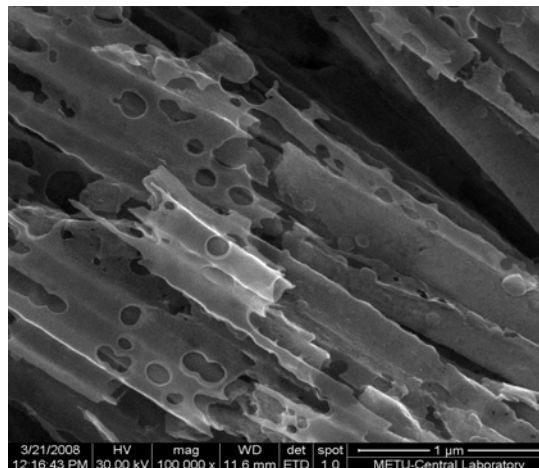
a



b



c



d

Fig. 2. SEM images of ordered LCMO nanowire arrays obtained at pH 3 after different dissolution times in 1 M NaOH a) 5 minutes b) 90 minutes c) 120 minutes at 14865X magnification d) 120 min. at 100000X magnification.

The sample was kept in NaOH until the AOO template had entirely dissolved to see individual LCMO nanowire images (Fig. 3), then the liberated nanowires were suspended in hexane. It was clearly observed that the nanowires were about 200 nm in diameter and 2.5 microns in length.

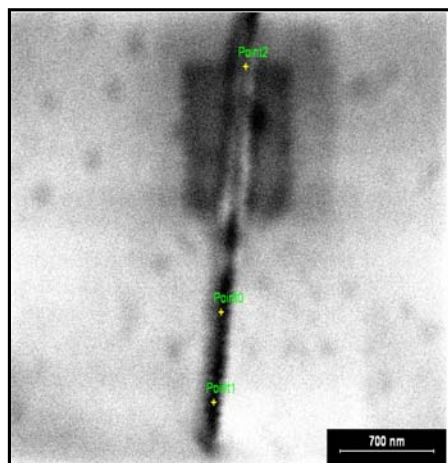


Fig. 3. EDX point analysis for $\text{La}_{0.75}\text{Ca}_{0.25}\text{MnO}_3$ nanowire arrays obtained at pH 3

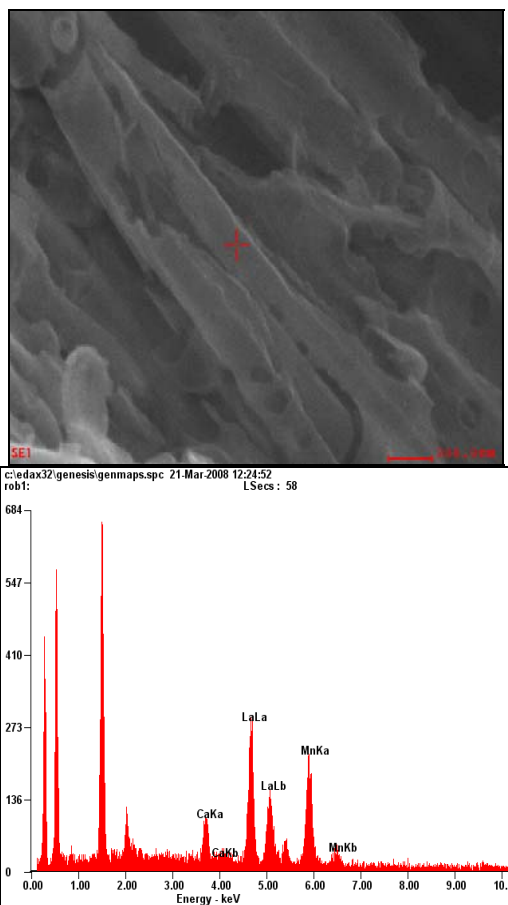


Fig. 4. A single $\text{La}_{0.75}\text{Ca}_{0.25}\text{MnO}_3$ nanowire

The average composition of the alloy nanowires was evaluated by EDX microanalysis (Fig. 4). The LCMO nanowire sample obtained at pH 3 showed the composition $\text{La}_{0.75}\text{Ca}_{0.25}\text{MnO}_3$.

Fig. 5 shows the XRD profiles for nanowire arrays within the AOO. As shown in Fig. 5, diffraction lines of cubic perovskite and Al_2O_3 are obtained for $\text{La}_{0.75}\text{Ca}_{0.25}\text{MnO}_3$ nanowire arrays within the AOO. The peaks observed at $2\theta = 32.58^\circ, 40.18^\circ, 46.78^\circ, 58.30^\circ, 68.60^\circ$ can be indexed as (121), (220), (202), (321), (242) reflections of $\text{La}_{0.75}\text{Ca}_{0.25}\text{MnO}_3$ cubic perovskite and the peaks also observed at $16.72^\circ, 25.40^\circ$ belong to $\gamma\text{-Al}_2\text{O}_3$.

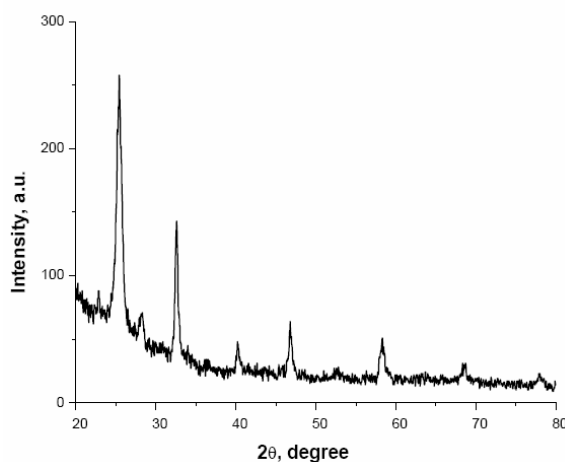


Fig. 5. XRD spectrum of $\text{La}_{0.75}\text{Ca}_{0.25}\text{MnO}_3$ nanowire arrays within the AOO

The hysteresis curves of the $\text{La}_{0.75}\text{Ca}_{0.25}\text{MnO}_3$ nanowire arrays obtained with the AOO template are shown in Fig. 6. The coercivities for nanowire arrays are 33 and 38 Oe for the applied field perpendicular to and parallel to the nanowire arrays, respectively. The magnetic signal was too low to be detected above the background noise by VSM for the nanowires produced at pH 2, pH 4, pH 5 and pH 6. It can be seen that magnetization curves of the nanowire arrays obtained at pH 3 are essentially identical for both magnetic field orientations, which indicates the isotropic magnetic nature of the $\text{La}_{0.75}\text{Ca}_{0.25}\text{MnO}_3$ nanowires deposited into the AOO template. It has been shown that ferromagnetic nanowires generally display perpendicular magnetic anisotropy due to their one dimensional character [26, 27]. Magnetic nanowires also show higher coercivity and remanent magnetization values when the magnetic field is applied along the direction out of plane with respect to the AOO template. On the other hand, it is well known that sometimes in polycrystalline materials the crystallites (nanograins, in the case of nanowires) can be oriented more or less at random, and the properties in various directions are not greatly different [28]. In the case of magnetic nanowires, the magnetocrystalline and shape anisotropies play important roles in the total magnetic anisotropy. The magnetization curves in Fig. 6 clearly

indicate that $\text{La}_{0.75}\text{Ca}_{0.25}\text{MnO}_3$ nanowire arrays obtained within the AAO template have no magnetic anisotropy. As previously suggested by Aravamudhan et al. [23, 26], this zero magnetic anisotropy could be related to two factors: 1) rough wire surfaces (see SEM pictures in Fig. 2) may reduce the shape anisotropy and 2) the random orientation of the nanograins in the $\text{La}_{0.75}\text{Ca}_{0.25}\text{MnO}_3$ magnetic nanowires may also lead to a nearly zero magnetocrystalline anisotropy, so the competition between shape and magnetocrystalline anisotropy may result in nearly zero magnetic anisotropy in $\text{La}_{0.75}\text{Ca}_{0.25}\text{MnO}_3$ magnetic nanowires, which is in agreement with some previously reported studies [21,23,26,29-31].

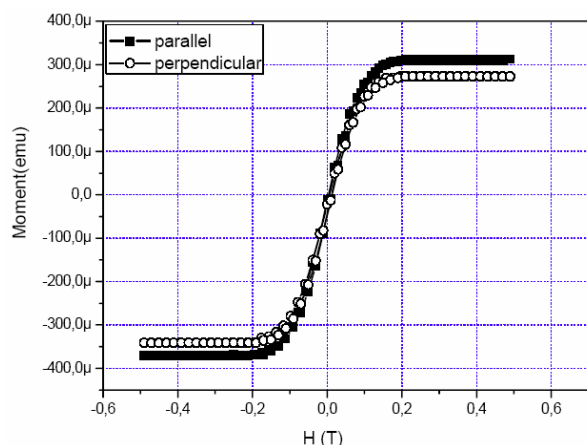


Fig. 6. M-H loops of LaCaMnO nanowire arrays at room temperature. Magnetic field applied to (■) parallel (○) perpendicular to nanowire length.

$\text{La}_{0.75}\text{Ca}_{0.25}\text{MnO}_3$ nanowires with ferromagnetic properties at room temperature are most desirable for applications in devices operating at room temperature. Shanthar et al. [9] have reported that $\text{La}_{0.67}\text{Ca}_{0.33}\text{MnO}_3$ nanowires with average diameter of 65 nm are ferromagnetic at room temperature and exhibit an enhanced ferromagnetic transition temperature well in excess of 300 K. It has been reported that the bulk polycrystalline $\text{La}_{0.75}\text{Ca}_{0.25}\text{MnO}_3$ composite has a Curie temperature of 224 K [1]. This study reports for the first time $\text{La}_{0.75}\text{Ca}_{0.25}\text{MnO}_3$ nanowires that show ferromagnetic properties at room temperature. The enhancement of the Curie temperature in the nanowire structure has been linked to the reduction of size. It was also proposed that the increase in the Curie temperature arises mainly from the hardening of the Jahn-Teller phonon mode as the size is reduced [9].

4. Conclusion

In this paper, we have successfully and for the first time produced ferromagnetic $\text{La}_{0.75}\text{Ca}_{0.25}\text{MnO}_3$ nanowires by the sol-gel template method inside porous Al_2O_3 . It

was observed from SEM micrographs that the nanowires are around 200 nm in diameter and 2.5 μm long. The magnetic properties of the nanowire arrays depend strongly on the pH of the solution. Magnetic characteristic of $\text{La}_{0.75}\text{Ca}_{0.25}\text{MnO}_3$ nanowire arrays produced at pH 3 shows no magnetic anisotropy, probably due to competition between shape and magnetocrystalline anisotropy.

Acknowledgment

This work was supported by Inonu University with project number I.U.BAP- 2008/64.

References

- [1] M. H. Phan, S. C. Yu, *J. Magn. Magn. Mater.* **308**, 325 (2007)
- [2] D. Toloman, G. Mihailescu, Al. Darabont, C. V. L. Pop, L. Olenic, A. Popa, O. Raita, M. Jivanescu, M. N. Grecu, L. M. Giurgiu, S. Idziak, S. K. Hoffmann, *J. Optoelectron. Adv. Mater.* **8**, 467 (2006)
- [3] H. Gencer, V. S. Kolat, S. Atalay, *Journal of Alloys and Compounds* **422**, 40 (2006)
- [4] H. Gencer, S. Atalay, H. I. Adiguzel, et al., *Physica B-Condensed Matter* **357**, 326 (2005)
- [5] S. Shingubara, O. Okino, *Solid- State Electron* **43**, 1143 (1999)
- [6] M. Li, C. Wang, *Sci. Bull.* **14**, 1172 (2001)
- [7] Y. Zhou, C. Shen, *Solid State Ionics* **146**, 81 (2002)
- [8] M. A. López-Quintela, L. E. Hueso, J. Rivas, F. Rivadulla, *Nanotechnology* **14**, 212 (2003)
- [9] K. Shanthar, S. Kar, A. K. Raychaudhuri, *Appl. Phys. Lett.* **84**, 993 (2004)
- [10] S. Chang, S. Yoon, H. Park, *Mater. Lett.* **53**, 432 (2002)
- [11] E. C. Walter, K. Ng, M. P. Zach, R. M. Penner, *Microelectron. Eng.* **61**, 555 (2002)
- [12] K. Nielsch, R. B. Wehrspohn, *Appl. Phys. Lett.* **79**, 1360 (2001)
- [13] X. Ma, H. Zhang, J. Xu, *Chem. Phys. Lett.* **363**, 579 (2002)
- [14] T. Zhang, C. G. Jin, T. Qian, X. L. Lu, J. M. Bai, X. G. Li, *J. Mater. Chem.* **14**, 2787 (2004)
- [15] F. Chen, H. W. Liu, K. F. Wang, H. Yu, S. Dong, X. Y. Chen, X. P. Jiang, Z. F. Ren, J. M. Liu, *J. Phys.: Condens. Matter.* **17**, L467 (2005)
- [16] C. N. R. Rao, A. Müller, A. A. K. Cheetham, *The Chemistry of Nanomaterials*, (Wiley-VCH, Weinheim, 2004)
- [17] M. Law, J. Goldberger, P. Yang, *Ann. Rev. Mater. Res.* **34**, 83 (2004)
- [18] R. Krahn, A. Yacoby, H. Shtrikman, I. Bar-Joseph, T. Dadoosh, J. Sperling, *Appl. Phys. Lett.* **81**, 730 (2002)
- [19] H. Chik, J. M. Xu, *Mater. Sci. Eng.* **R 43**, 103 (2004).

- [20] H. X. He, N. J. Tao, *Encyclopedia of Nanoscience and Nanotechnology*, (American Scientific Publishers, New York, 2004)
- [21] D. J. Sellmyer, M. Zheng, R. Skomski, *J. Phys. Condens. Matter* **13**, R433 (2001)
- [22] F. E. Atalay, H. Kaya, S. Atalay, S. Tari, *Journal of Alloys and Compounds* **469**, 458 (2009)
- [23] S. Aravamudhan, K. Luongo, P. Poddar, H. Srikanth, S. Bhansali, *Appl. Phys. A* **87**, 773 (2007)
- [24] J. Wang, A. Manivannan, N. Q. Wu, *Thin Solid Films* **517**, 582 (2008).
- [25] H. Masuda, K. Fukuda, *Science* **268**, 1466 (1995)
- [26] S. Aravamudhan, J. Singleton, P. A. Goddard, S. Bhansali, *J. Phys. D: Appl. Phys.* **42**, 115008 (2009).
- [27] L. Sun, Y. Hao, C. Chien, P. Searson, *IBM Journal of Research and Development* **49**, 79 (2005)
- [28] R. M. Bozorth, *Ferromagnetism*, (IEEE Press, Livre, 1993)
- [29] S. Ge, C. Li, X. Ma, W. Li, L. Xi, C. X. Li, *J. Appl. Phys.* **90**, 509 (2001)
- [30] A. Kumar, S. Fähler, H. Schlörb, K. Leisiner, L. Schultz, *Phys. Rev. B* **73**, 064421 (2006)
- [31] M. Vázquez, K. Pirota, J. Torrejón, D. Navas, M. Hernández-Vélez, *J. Magn. Magn. Mater.* **294**, 174 (2005)

*Corresponding author: fatalay@inonu.edu.tr